

# Thermal biphotons

Ohad Lib, Yaron Bromberg\*

Racah Institute of Physics, The Hebrew University of Jerusalem, Jerusalem, 91904 Israel

\*To whom correspondence should be addressed; E-mail: Yaron.Bromberg@mail.huji.ac.il.

**The observation of the Hanbury Brown and Twiss (HBT) effect with thermal light marked the beginning of a new era in the field of optical coherence. To date, all types of thermal light sources that were considered consisted of independent emitters that emit uncorrelated photons. In this work, we study a new class of thermal light, coined *thermal biphotons*, in which the independent emitters emit pairs of correlated photons. We show that for thermal biphotons, the width of the HBT peak is remarkably different than the size of their coherence area, leading to violation of the Siegert relation and a breakdown of the speckle-fluctuations interpretation. We derive a new separability criterion based on a disordered averaged measurement of the width of the HBT peak and certify spatial entanglement in our state. We further provide an alternative interpretation of the results based on a connection between the HBT effect and coherent backscattering of light. Beyond reflecting new insights on the coherence properties of thermal light in the presence of spatial correlations, our work opens the door for the certification and quantification of spatial entanglement using disordered averaged measurements.**

## Introduction

One of the most important steps towards our modern understanding of optical coherence was the observation of the Hanbury Brown and Twiss (HBT) effect, in which the size of a thermal light source was inferred using intensity correlation measurements between two detectors (1, 2). Although being completely consistent with the classical theory of light, the observation of the HBT effect triggered a heated debate on the quantum nature of photons (3). The full quantum description of the HBT effect was finally given by Glauber in his seminal work on the quantum theory of optical coherence (4, 5), marking the birth of the field of quantum optics. Following these results, second-order coherence (or intensity interferometry) has gained significant importance in the field of quantum optics, playing a major role in phenomena such as Hong-Ou-Mandel interference (6) and the characterization of single and entangled photon sources (7, 8).

In all demonstrators to date of the spatial HBT effect, the sources were spatially incoherent thermal sources, which are modeled by a large number of independent emitters that emit uncorrelated photons (Fig.1(a)) (9). For such sources, the classical interpretation of fluctuating Gaussian fields, and the quantum interpretation of photon bunching, predict exactly the same features of the HBT effect: the second order coherence exhibits a 2:1 peak-to-background ratio with a width that is inversely proportional to the source size. Similarly, it is generally believed that the Gaussian fields description of thermal ghost imaging yields equivalent results to the quantum theory (10–15). An intriguing question is whether the equivalence between the Gaussian field and the photon bunching interpretations holds for other types of incoherent sources. To study this question, we introduce a new class of spatially incoherent sources, thermal biphotons, that are made of independent emitters that emit *pairs* of photons. Beyond reflecting new insights on the classical and quantum description of spatial coherence in the presence of two-

photon correlations, understanding the coherence properties of thermal biphotons may open the door for new applications of two-photon sources with low spatial coherence.

In this work, we theoretically and experimentally study the coherence properties of thermal biphotons and their close relation to spatial entanglement and correlations. We show that thermal biphotons exhibit a 2:1 HBT peak, as in the standard HBT effect, indicating their thermal nature. The width of the HBT peak, however, is different for thermal biphotons. We show that in contrast to the standard HBT effect with thermal light, for thermal biphotons the quantum and classical pictures are not equivalent. They predict different widths for the HBT peak, leading to violation of the Siegert relation and to the breakdown of the fluctuating-speckle interpretation of the HBT effect. We further show that the width of the HBT peak of thermal biphotons can be utilized as a tool for certifying the existence of spatial entanglement in the quantum state. Finally, we give an alternative interpretation of the observed results by unveiling a relation between the HBT effect and coherent backscattering of light (CBS) in complex media.

## Results

### Thermal biphotons and the HBT effect

We begin by briefly describing the standard HBT effect with thermal light. Light from a thermal source of size  $D$  is measured at the far-field using two detectors at angular separation  $\Delta\theta$  relative to the source (Fig.1(a)). Since the thermal light field has Gaussian statistics, the instantaneous intensity distribution at the detectors' plane exhibits rapidly fluctuating speckle patterns (16, 17). If the two detectors lie within the same speckle grain, their intensities fluctuate correlatively, and  $g^{(2)}(\Delta\theta) \approx \frac{\langle I^2 \rangle}{\langle I \rangle^2} = 2$ , where the last equality results from the exponential statistics of thermal light (18). Otherwise, the detectors measure intensities at uncorrelated speckle grains, yielding  $g^{(2)}(\Delta\theta) = 1$ . The width of the 2:1 peak in  $g^{(2)}(\Delta\theta)$  is thus determined by the speckle grain size, which scales like  $\Delta\theta \propto \lambda/D$ , where  $\lambda$  is the wavelength of the

thermal light. An equivalent classical view of the HBT effect is given by utilizing the Siegert relation,  $g^{(2)}(\Delta\theta) = 1 + |g^{(1)}(\Delta\theta)|^2$ , which connects the first- and second-order coherence functions of thermal light (19). According to the Van Cittert-Zernike theorem (9), the width of the first-order coherence function  $g^{(1)}(\Delta\theta)$  is determined by the Fourier transform of the intensity of the thermal source. Therefore, using Siegert's relation, one again finds that the width of the HBT peak is the same, and scales as  $\Delta\theta \propto \lambda/D$ . The quantum description of the thermal HBT effect yields the exact same results as the above classical interpretation. In the framework of quantum mechanics, one has to sum all different two-photon amplitudes leading to a detection of a photon in each detector (20). The paths corresponding to two such amplitudes are illustrated in Fig.1(a). Indeed, if the distance between the detectors is small enough, the different amplitudes add coherently, leading to an increase in intensity correlations.

Next, we consider the case of thermal biphotons, in which a source of size  $D$  is comprised of two-photon emitters, each having a characteristic size of  $d$  (Fig.1(b)). Inspired by our experimental implementation described later, we model a source of thermal biphotons using a quantum state of the form  $|\psi\rangle = \int dr_s dr_i \sqrt{P(r_s, r_i)} \exp(i(\Phi(r_s, r_i))) \exp(i(\phi(r_s) + \phi(r_i))) |1_{r_s}, 1_{r_i}\rangle$ , where  $|1_{r_s}, 1_{r_i}\rangle$  is a Fock state describing the emission of two photons (coined signal and idler photons) at positions  $r_s$  and  $r_i$ .  $\sqrt{P(r_s, r_i)} \exp(i(\Phi(r_s, r_i)))$  is a general polar representation of the distribution of the emitted photons, which is symmetric to the exchange of the two photons, and the relative phase between different two-photon emission  $\phi(r_s) + \phi(r_i)$  is assumed to randomly fluctuate in space and time. We quantitatively define the characteristic size of the two-photon emitters as the width of the correlations between the photons at the plane of the source,  $d^2 \equiv \int dr_s dr_i (r_s - r_i)^2 P(r_s, r_i)$ , yielding that  $d$  is  $\sqrt{2}$  times the standard deviation of the two-photon distance distribution  $h_-(r_-) \equiv \int dr_+ P(r_s, r_i)$ , where  $r_{\pm} = (r_i \pm r_s)/\sqrt{2}$  (see Supplementary information). Similarly, the characteristic size of the source,  $D$ , is defined as the standard deviation of the marginal single-photon distribution

$h_s(r_s) \equiv \int dr_i P(r_s, r_i) = \langle \psi | a_s^\dagger(r_s) a_s(r_s) | \psi \rangle$ , where  $a_s^\dagger(r_s)$  is the creation operator of a signal photon at position  $r_s$  at the plane of the source.

Using this model, we can now derive the expression for the second-order coherence function of thermal biphotons (see Supplementary information):

$$g^{(2)}(\Delta\theta) = \frac{\langle \psi | a_s^\dagger(\theta_1) a_i^\dagger(\theta_2) a_i(\theta_2) a_s(\theta_1) | \psi \rangle}{\langle \psi | a_s^\dagger(\theta_1) a_s(\theta_1) | \psi \rangle \langle \psi | a_i^\dagger(\theta_2) a_i(\theta_2) | \psi \rangle} = 1 + \widetilde{h}_-(\sqrt{2}k\Delta\theta) \quad (1)$$

where  $k$  is the wavenumber,  $a_s(\theta) = \sqrt{(k/2\pi)} \int dr_s a_s(r_s) \exp(-ik\theta r_s)$  is the annihilation operator for a signal photon with (paraxial) transverse wavevector  $q = k\theta$  at the plane of the source and  $\widetilde{h}_-(k\Delta\theta)$  is the Fourier transform of the two-photon distance distribution  $h_-(r_-)$ . The first-order coherence function can be evaluated as well, yielding  $g^{(1)}(\Delta\theta) = \widetilde{h}_s(k\Delta\theta)$ , where  $\widetilde{h}_s(k\Delta\theta)$  is the Fourier transform of  $h_s(r_s)$ , in accordance with the Van Cittert-Zernike theorem. For a separable quantum state, corresponding to a standard thermal source without correlations,  $P(r_s, r_i)$  can be written as  $P(r_s, r_i) = P_1(r_s)P_1(r_i)$ . In this case, Eq.(1) captures the standard thermal HBT effect, namely, the Siegert relation holds  $g^{(2)}(\Delta\theta) = 1 + |\widetilde{h}_s(k\Delta\theta)|^2$ . Thus for separable states, the width of  $g^{(2)}(\Delta\theta)$  is proportional to the width of  $\widetilde{h}_s(k\Delta\theta)$ , and  $\Delta\theta_{HBT} \propto \lambda/D$ .

For thermal biphotons, described by a non-separable state, the photons exhibit spatial correlations, such that the size of the two-photon emitters is smaller than the total size of the source ( $d < D$ ). As the width of  $h_-(r_-)$  is determined by  $d$ , the width of the HBT peak corresponds to  $\Delta\theta_{HBT} \propto \lambda/d$  for thermal biphotons, yielding an HBT peak which is  $D/d$  times wider relative to thermal light. In contrast, the width of the first-order coherence function is still determined by the width of the source,  $D$ , and is not affected by the size of the two-photon emitters. These results show that in the case of thermal biphotons, the classical picture of a fluctuating speckle pattern for the HBT effect collapses, and the Siegert relation is broken.

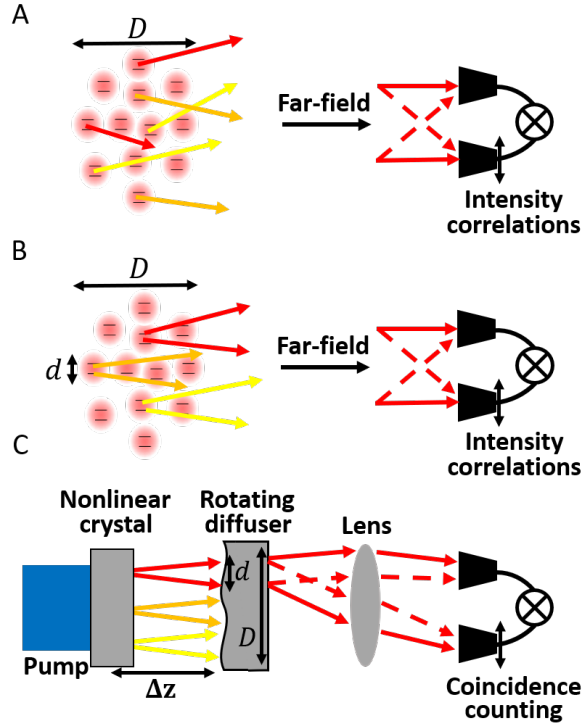


Figure 1: (a) Illustration of an HBT measurement with a thermal source of size  $D$ . Photons are emitted by uncorrelated emitters distributed over the entire source. (b) Illustration of an HBT measurement with thermal biphotons. Pairs of photons are emitted by two-photon emitters of size  $d$ . (c) Experimental implementation of a pseudo-thermal biphoton source. Pairs of correlated photons generated by spontaneous parametric down conversion are scattered by a rotating diffuser.

## Experimental realization of pseudo-thermal biphotons

To experimentally study the coherence features of thermal biphotons, we realize thermal biphotons using scattering of spatially entangled photons by a rotating diffuser. Scattering of spatially entangled photons exhibits a wide range of effects, such as two-photon speckle patterns (21–24) and the observation of bosonic, fermionic, and anyonic symmetries (25). Here, in analogy with the creation of pseudo-thermal light by a laser beam and a rotating diffuser (26), we utilize scattering of spontaneous parametric down converted light to create a source of pseudo-thermal biphotons and study their coherence properties. This is in contrast to previous studies that

considered coherence properties of entangled photons produced using either a coherent or an incoherent pump beam, yet without dynamic scattering (27–30).

A simplified illustration of the experimental setup is presented in Fig.1(c). Spatially entangled photons are created via type 1 spontaneous parametric down conversion (SPDC), by pumping a 8 mm long nonlinear Beta Barium Borate (BBO) crystal with a continuous-wave pump beam ( $\lambda = 404 \text{ nm}$ ). The twin photons are phase-randomized by passing through a rotating diffuser. The second-order coherence function is measured at the far-field using two single-photon detectors and a coincidence counting circuit (Swabian Time Tagger). In the experiment, one detector is always kept stationary at  $\theta_i = 0$  while the other scans the angle  $\theta_s$ . A polarizer and 80 nm bandpass filters (not shown) are used to select the wavelength and polarization of the measured photons. The width of the two-photon emitter,  $d$ , which in our setup is determined by the distance between the signal and idler photons at the plane of the diffuser, can be tuned by changing the distance  $\Delta z$  between the nonlinear crystal and the rotating diffuser.

In our experiment, we tune the size of the two-photon emitters such that  $D \approx 2d$ , by setting  $\Delta z = 35 \text{ mm}$ . The second-order coherence function  $g^{(2)}(\Delta\theta)$  exhibits an 2:1 HBT peak (black dots), yet its width is determined by the size of the two-photon emitters rather than by the total width of the source. To study the relation between the first- and second-order coherence functions, we measure the intensity distribution of the source at the diffuser's plane using a CMOS camera, and compute its Fourier transform to obtain  $g^{(1)}(\Delta\theta)$  according to the Van Cittert-Zernike theorem (9). We thus observe  $1 + |g^{(1)}(\Delta\theta)|^2$  (blue triangles). A clear violation of Siegert's relation is observed, as the widths of the two peaks are significantly different, supporting the theoretical prediction of Eq.(1).

Thus far, we have shown that the width of the HBT peak for thermal biphotons is determined by the size of the two-photon emitter  $d$  rather than by the size of the entire source  $D$ , i.e.  $\Delta\theta_{HBT} \propto \lambda/d$ . From the classical speckle interpretation of the HBT effect with thermal light,

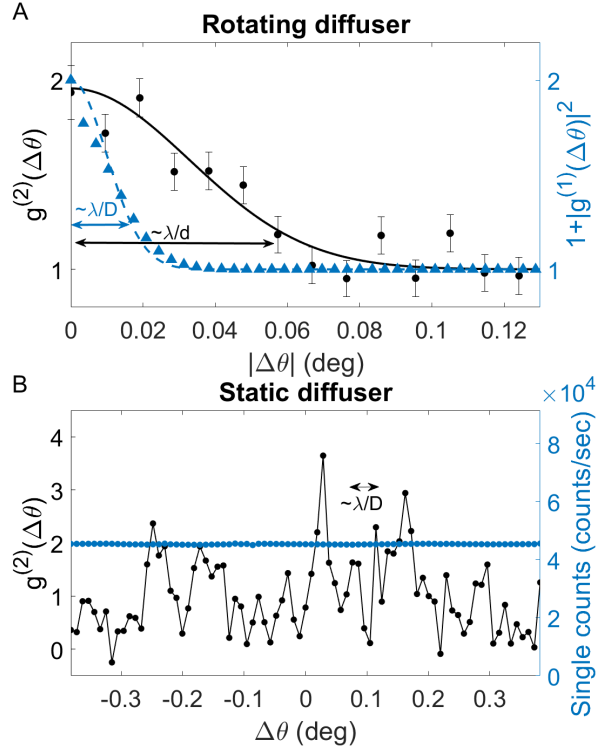


Figure 2: (a) Second-order  $g^{(2)}(\Delta\theta)$  and first-order  $g^{(1)}(\Delta\theta)$  coherence measurements of thermal biphotons. The data is taken with  $\Delta z = 35$  mm ( $D \approx 2d$ ). We use the double-Gaussian approximation of SPDC and apply it to the theory of thermal biphotons to derive an explicit and simple model for the results (31, 32). We obtain the following approximations for the coherence functions of thermal biphotons,  $g_{DG}^{(2)}(\Delta\theta) = 1 + \exp(-(d^2(k\Delta\theta)^2)/2)$  and  $|g_{DG}^{(1)}(\Delta\theta)|^2 = \exp(-D^2(k\Delta\theta)^2)$  (see Supplementary information). We apply this model for the observed results for the first- and second-order coherence functions (dashed and solid curves, respectively), yielding  $d = 230 \pm 16\mu\text{m}$  and  $D = 525 \pm 2\mu\text{m}$ . (b) The  $g^{(2)}(\Delta\theta)$  measurement with a static diffuser at  $\Delta z = 35$  mm ( $D \approx 2d$ , black) exhibits a two-photon speckle with a typical speckle size of  $\lambda/D$ . The single photon counts (blue) are homogeneously distributed and do not exhibit a speckle pattern. In all  $g^{(2)}(\Delta\theta)$  measurements, accidental counts are subtracted.

where the width of the HBT peak is equal to the width of a speckle grain  $\Delta\theta_{\text{speckle}} \propto \lambda/D$ , one might expect that for thermal biphotons the width of the HBT peak will be equal to the width of the two-photon speckle grain. We thus examine the two-photon speckle pattern obtained by measuring the second-order coherence function for a static diffuser (Fig.2(b)). Since in SPDC the single photon distribution is spatially incoherent, no speckle pattern is observed in

the intensity measurement, even though the diffuser is static (blue dots) (22, 24). Nevertheless, the two-photon wavefunction is spatially coherent, thus exhibiting a two-photon speckle pattern (black dots). The width of a two-photon speckle grain is  $\Delta\theta_{speckle} \propto \lambda/D$  (22), which in contrast to the standard HBT effect, is not the same as the width of the HBT peak. Thus, we show that in contrast to the standard HBT effect, for thermal biphotons the quantum and the classical speckle-based interpretations are not equivalent, as the width of the HBT peak is different from the speckle size.

## The role of spatial entanglement

For thermal biphotons, we have shown that the width of the HBT peak at the far-field is determined by the near-field correlations at the plane of the diffuser. Since the near field correlations do not necessarily have to be quantum, breakdown of the Siegert relation does not imply immediately that thermal biphotons are non-classical. Nevertheless, simultaneous observation of a wide HBT peak and narrow momentum correlations, measured at the far-field of the diffuser, can be used to certify entanglement between the photons impinging onto the rotating diffuser.

To prove this claim, we use Mancini's separability criterion for the signal and idler photons before hitting the diffuser (33, 34). If the signal and idler photons are in a separable state, the criteria sets a lower bound for the product of the uncertainty in their mean transverse momentum  $\sigma_{k\theta_s+k\theta_i}$ , and the uncertainty in their relative positions  $\sigma_{r_s-r_i}$ ,  $\sigma_{k\theta_s+k\theta_i}^2 \sigma_{r_s-r_i}^2 \geq 1$ . The uncertainty in the mean transverse momentum  $\sigma_{k\theta_s+k\theta_i}$  can be measured by the width of the far-field coincidence distribution in the absence of the diffuser (34). To relate the uncertainty in the relative positions  $\sigma_{r_s-r_i}$  to the HBT peak, we consider the most general two-photon separable state which exhibits a 2:1 HBT peak (see Supplementary),  $\rho = \sum_l p_l |\chi_l\rangle \langle \chi_l|_{signal} \otimes |\chi_l\rangle \langle \chi_l|_{idler}$ , where  $\sum_l p_l = 1$ . Writing  $|\chi_l\rangle = \int dr u_l(r) |1_r\rangle$ , we obtain from Eq.(1) that the HBT peak is  $g^{(2)}(\Delta\theta) - 1 = \sum_l p_l \left| \int dr |u_l(r)|^2 \exp(-i\Delta\theta kr) \right|^2$ . Looking at its Fourier transform, we obtain

$F_{HBT}(r) = \sum_l p_l |u_l(r)|^2 * |u_l(-r)|$ , where  $*$  denotes convolution. We find that  $\sigma_{FHBT}$ , the width of  $F_{HBT}(r)$ , equals the uncertainty in the relative positions of the signal and idler, i.e.  $\sigma_{FHBT}^2 = \sigma_{r_s - r_i}^2$ . Entanglement can therefore be certified by observing

$$\sigma_{FHBT}^2 \sigma_{k\theta_s + k\theta_i}^2 < 1 \quad (2)$$

Since both the HBT peak and the uncertainty in the mean transverse momentum  $\sigma_{k\theta_s + k\theta_i}$  are measured in the same plane, the entanglement certification criteria we derived does not require measurements in both the near-field and far-field planes as in the standard entanglement criteria (34). Instead, we replace the near-field measurements with an disorder-averaged far-field measurement.

To demonstrate the application of our criterion to the case of the double-Gaussian approximation of SPDC described earlier, we plot  $\ln(\sigma_{FHBT}^2 \sigma_{k\theta_s + k\theta_i}^2)$  as a function of the normalized distance between the crystal and the rotating diffuser, and the Schmidt number (Fig.3). In our experiment, for  $\Delta z = 35\text{mm}$ , we obtain  $\sigma_{FHBT}^2 \sigma_{k\theta_s + k\theta_i}^2 = 0.71 \pm 0.04$ , certifying the spatial entanglement in the quantum state.

To relate this result to the fluctuating-speckle interpretation, we note that the typical size of a speckle grain observed with a static diffuser cannot be smaller than a diffraction limited spot at the far-field (16). Therefore, our separability criterion suggests that the simultaneous observation of a wide HBT peak (corresponding to a small  $\sigma_{FHBT}$ ) and a narrow speckle grain is not possible without the presence of spatial entanglement.

## Coherent backscattering in the advanced wave picture

While we have showed that the fluctuating-speckle interpretation fails to describe the coherence properties of thermal biphotons, we give an alternative classical interpretation that is surprisingly related to coherent backscattering of light (CBS) (35). By virtue of Klyshko's advanced

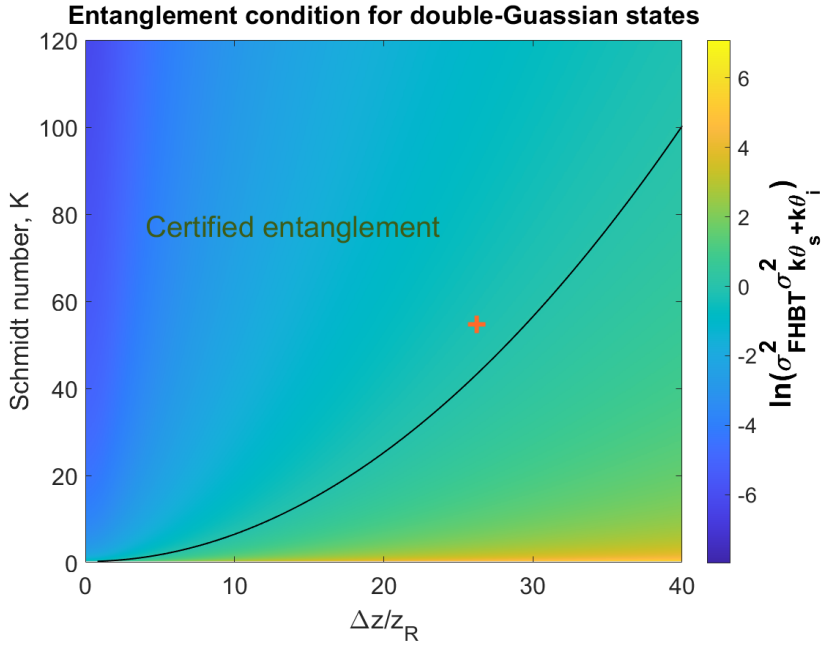


Figure 3: Theoretical plot of the entanglement criterion for thermal biphotons under the double-Gaussian approximation. The product  $\sigma_{FHBT}^2 \sigma_{k\theta_s + k\theta_i}^2$  depends on the distance between the nonlinear crystal and the rotating diffuser, and the Schmidt number. The distance is normalized by the Rayleigh range for a beam of width  $d$  at the crystal's plane, which is in turn determined by the length of our crystal,  $L = 8\text{mm}$ . The Schmidt number is varied by changing the waist of the pump beam. The threshold for entanglement certification, according to Eq.(2), is marked by a black line. An orange + sign marks our approximated experimental conditions.

wave picture, one of the single-photon detectors can be replaced with an equivalent classical source, the nonlinear crystal acts as a mirror, and the coincidence measurement can be replaced by measuring the intensity at the plane of the second detector (36). Illustration of the equivalent advanced wave picture setup for our experiment is presented in the inset of Fig.4, where a classical, well-collimated, beam propagates through a diffuser-mirror-diffuser configuration, and measured at the far-field of the diffuser. This configuration exhibits coherent backscattering (CBS), in which an enhanced disorder-averaged intensity is observed in the backscattered direction, due to the constructive interference of reciprocal paths (35, 37). Two such paths are illustrated in the inset of Fig.4 (solid and dashed red arrows). Each of the paths exits the

effective scattering medium at the entry point of the other and are therefore reciprocal when measuring at  $\Delta\theta = 0$ . The mean transverse distance between the entry and exit points of the paths corresponds to an effective transport mean free path, given by  $l = \langle |r_{in} - r_{out}| \rangle$ , where  $r_{in}$  and  $r_{out}$  are the transverse positions of the entry and exit points respectively. The intensity in the backscattered direction relative to the background is twice as large, as in the HBT effect. The width of the CBS peak is determined by the effective transport mean free path, which is equivalent to the two-photon emitter size  $d$ , thus explaining the width of the HBT peak of thermal biphotons. To experimentally demonstrate the connection between thermal biphotons and coherent backscattering of a laser beam, we have measured the CBS peak obtained for  $\Delta z = 35\text{mm}$  (Fig.4, black). The curve is fitted according to the double-Gaussian approximation discussed above, yielding  $d = 264 \pm 1\mu\text{m}$ . In addition, we measure the speckle pattern observed with a static diffuser in the advanced wave picture, demonstrating that the width of the CBS peak is indeed larger than the width of a speckle grain (Fig.4, blue)

## Conclusion

We presented a new type of thermal light, coined thermal biphotons, in which the photons are emitted in pairs from independent emitters. We have shown both theoretically and experimentally that in contrast to the standard HBT effect, the width of the HBT peak for thermal biphotons is determined by the size of the two-photon emitters rather than by the total size of the source. Therefore, we obtain that the width of the HBT peak can be wider than the speckle size. As a result, we observe a clear violation of the Siegert relation. Furthermore, we discuss the role of spatial entanglement in the observed result, deriving the first separability criterion based on a measurement in a disordered averaged basis. We experimentally break the separability criterion, certifying the existence of spatial entanglement in our state and explaining the breakdown of the fluctuating-speckle interpretation. Finally, we use the advanced wave

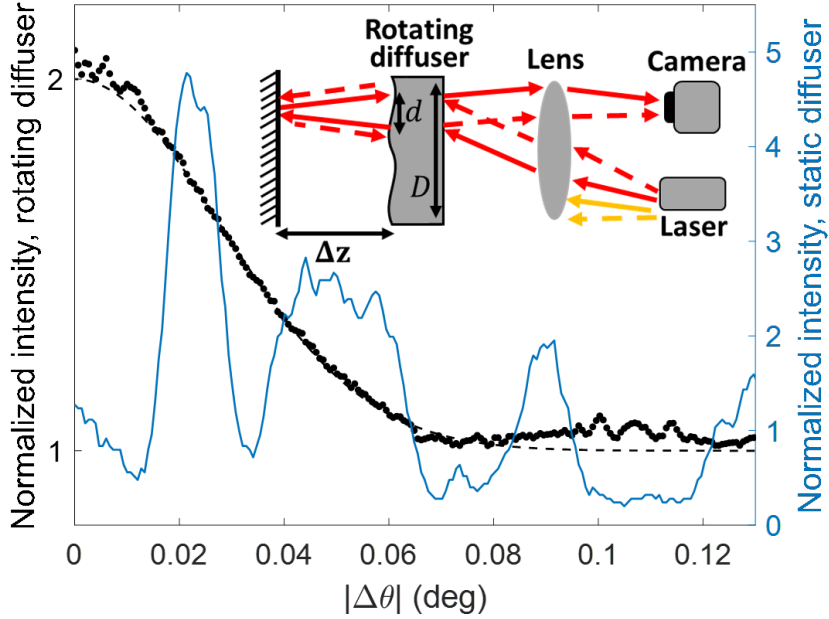


Figure 4: Illustration of the advanced wave picture setup is presented in the inset. One of the single-photon detectors is replaced with a laser, illuminating a diffuser-mirror-diffuser configuration. The intensity distribution is recorded at the far-field for  $\Delta z = 35\text{mm}$ . An enhanced backscattering is observed for a measurement with a rotating diffuser (black dots), which is presented together with a theoretical fit to the double-Gaussian model. For a static diffuser, a speckle pattern is observed (blue line).

picture interpretation of our experiment to demonstrate a connection between the HBT effect and coherent backscattering. We believe that further studies of this new class of thermal light can lead to future applications. For example, inspired by classical imaging schemes that utilize pseudo-thermal light for structured illumination and speckle-free imaging (15, 38–44), it would be intriguing to consider thermal biphotons for structured illumination quantum imaging. In addition, our HBT peak-based separability criterion might open new avenues in the developing field of entanglement quantification and certification (45–47).

## References

1. R. H. Brown, R. Q. Twiss, *Nature* **178**, 1046 (1956).

2. R. H. Brown, R. Q. Twiss, *Nature* **177**, 27 (1956).
3. E. Brannen, H. I. Ferguson, *Nature* **178**, 481 (1956).
4. R. J. Glauber, *Physical Review Letters* **10**, 84 (1963).
5. R. J. Glauber, *Physical Review* **130**, 2529 (1963).
6. C.-K. Hong, Z.-Y. Ou, L. Mandel, *Physical review letters* **59**, 2044 (1987).
7. P. G. Kwiat, *et al.*, *Physical Review Letters* **75**, 4337 (1995).
8. C. Kurtsiefer, S. Mayer, P. Zarda, H. Weinfurter, *Physical review letters* **85**, 290 (2000).
9. J. W. Goodman, *Statistical optics* (John Wiley & Sons, 2015).
10. A. Gatti, E. Brambilla, M. Bache, L. A. Lugiato, *Physical review letters* **93**, 093602 (2004).
11. G. Scarcelli, V. Berardi, Y. Shih, *Physical review letters* **96**, 063602 (2006).
12. A. Gatti, M. Bondani, L. Lugiato, M. Paris, C. Fabre, *Physical review letters* **98**, 039301 (2007).
13. J. H. Shapiro, *Physical Review A* **78**, 061802(R) (2008).
14. B. I. Erkmen, J. H. Shapiro, *Physical Review A* **77**, 043809 (2008).
15. Y. Bromberg, O. Katz, Y. Silberberg, *Physical Review A* **79**, 053840 (2009).
16. J. W. Goodman, *Speckle phenomena in optics: theory and applications* (Roberts and Company Publishers, 2007).
17. A. Aspect, *arXiv preprint arXiv:2005.08239* (2020).

18. M. O. Scully, M. S. Zubairy, *Quantum optics* (American Association of Physics Teachers, 1999).
19. A. Siegert, *On the fluctuations in signals returned by many independently moving scatterers* (Radiation Laboratory, Massachusetts Institute of Technology, 1943).
20. U. Fano, *American Journal of Physics* **29**, 539 (1961).
21. C. Beenakker, J. Venderbos, M. Van Exter, *Physical review letters* **102**, 193601 (2009).
22. W. Peeters, J. Moerman, M. Van Exter, *Physical review letters* **104**, 173601 (2010).
23. A. Klein, O. Agam, B. Spivak, *Physical Review A* **94**, 013828 (2016).
24. O. Lib, G. Hasson, Y. Bromberg, *Science Advances* **6**, eabb6298 (2020).
25. M. van Exter, J. Woudenberg, H. D. L. Pires, W. Peeters, *Physical Review A* **85**, 033823 (2012).
26. F. T. Arecchi, *Physical Review Letters* **15**, 912 (1965).
27. A. Joobeur, B. E. Saleh, T. S. Larchuk, M. C. Teich, *Physical Review A* **53**, 4360 (1996).
28. B. E. Saleh, A. F. Abouraddy, A. V. Sergienko, M. C. Teich, *Physical Review A* **62**, 043816 (2000).
29. H. Defienne, S. Gigan, *Physical Review A* **99**, 053831 (2019).
30. W. Zhang, R. Fickler, E. Giese, L. Chen, R. W. Boyd, *Optics express* **27**, 20745 (2019).
31. C. Law, J. Eberly, *Physical review letters* **92**, 127903 (2004).
32. S. P. Walborn, C. Monken, S. Pádua, P. S. Ribeiro, *Physics Reports* **495**, 87 (2010).

33. S. Mancini, V. Giovannetti, D. Vitali, P. Tombesi, *Physical review letters* **88**, 120401 (2002).
34. J. C. Howell, R. S. Bennink, S. J. Bentley, R. W. Boyd, *Physical Review Letters* **92**, 210403 (2004).
35. E. Akkermans, P. Wolf, R. Maynard, *Physical review letters* **56**, 1471 (1986).
36. D. Klyshko, *Soviet Physics Uspekhi* **31**, 74 (1988).
37. E. Jakeman, *JOSA A* **5**, 1638 (1988).
38. D. Lim, K. K. Chu, J. Mertz, *Optics letters* **33**, 1819 (2008).
39. E. Mudry, *et al.*, *Nature Photonics* **6**, 312 (2012).
40. B. Redding, G. Allen, E. R. Dufresne, H. Cao, *Applied optics* **52**, 1168 (2013).
41. J.-E. Oh, Y.-W. Cho, G. Scarcelli, Y.-H. Kim, *Optics letters* **38**, 682 (2013).
42. F. V. Pepe, *et al.*, *Physical review letters* **119**, 243602 (2017).
43. T. Gregory, P.-A. Moreau, E. Toninelli, M. J. Padgett, *Science advances* **6**, eaay2652 (2020).
44. H. Defienne, B. Ndagano, A. Lyons, D. Faccio, *Nature Physics* pp. 1–7 (2021).
45. J. Bavaresco, *et al.*, *Nature Physics* **14**, 1032 (2018).
46. N. Friis, G. Vitagliano, M. Malik, M. Huber, *Nature Reviews Physics* **1**, 72 (2019).
47. N. H. Valencia, *et al.*, *Quantum* **4**, 376 (2020).

## **Acknowledgments**

We acknowledge support from the Zuckerman STEM Leadership Program and Israel Science Foundation (grant No. 1268/16).

## **Supplementary materials**

Supplementary Text

Fig. S1

## Supplementary Text

### Quantum state of thermal biphotons generated via SPDC

In this section, we provide a model for the quantum state of the thermal biphotons generated in our experiment. At the plane of the nonlinear crystal, the quantum state of the generated biphotons is(32)

$$|\psi\rangle = \int d\mathbf{q}_s d\mathbf{q}_i v(\mathbf{q}_s + \mathbf{q}_i) A(\mathbf{q}_s, \mathbf{q}_i) |1_{\mathbf{q}_s}, 1_{\mathbf{q}_i}\rangle \quad (S1)$$

where  $A(\mathbf{q}_s, \mathbf{q}_i) = \text{sinc}\left(\mu_{oo} + l_t(q_{sx} + q_{ix}) + \frac{L}{4k_p}(\mathbf{q}_s - \mathbf{q}_i)^2\right) \exp(-il_t(q_{sx} + q_{ix}))$  is the phase matching function for a type 1 SPDC process for degenerate photons with a crystal of length  $L$ , a walk-off length  $l_t$  and a pump wavevector  $k_p$  inside the crystal.  $\mu_{oo}$  is a constant determined by the angle of the nonlinear crystal relative to the pump beam,  $v(\mathbf{q})$  is the angular spectrum of the pump beam, which also includes the normalization constant for the state, and  $|1_{\mathbf{q}_s}, 1_{\mathbf{q}_i}\rangle$  describes a state of signal and idler photons with transverse wavevectors  $\mathbf{q}_s$  and  $\mathbf{q}_i$ .

Under paraxial propagation of distance  $\Delta z$ , the quantum state becomes (32)

$$|\psi\rangle = \int d\mathbf{q}_s d\mathbf{q}_i v(\mathbf{q}_s + \mathbf{q}_i) A(\mathbf{q}_s, \mathbf{q}_i) \exp\left(-\frac{i\Delta z}{2k}(\mathbf{q}_i^2 + \mathbf{q}_s^2)\right) |1_{\mathbf{q}_s}, 1_{\mathbf{q}_i}\rangle \quad (S2)$$

where  $k$  is the wavenumber of the entangled photons.

The state  $|\psi\rangle$  can be represented in the spatial domain using the Fourier transform (FT) of the two-photon amplitude  $f(\mathbf{r}_s, \mathbf{r}_i) = \text{FT}\left[v(\mathbf{q}_s + \mathbf{q}_i) A(\mathbf{q}_s, \mathbf{q}_i) \exp\left(-\frac{i\Delta z}{2k}(\mathbf{q}_i^2 + \mathbf{q}_s^2)\right)\right]$ . Using the polar representation of  $f(\mathbf{r}_s, \mathbf{r}_i) = \sqrt{P(\mathbf{r}_s, \mathbf{r}_i)} \exp(i(\Phi(\mathbf{r}_s, \mathbf{r}_i)))$  we obtain:

$$|\psi\rangle = \int d\mathbf{r}_s d\mathbf{r}_i \sqrt{P(\mathbf{r}_s, \mathbf{r}_i)} \exp(i(\Phi(\mathbf{r}_s, \mathbf{r}_i))) |1_{\mathbf{r}_s}, 1_{\mathbf{r}_i}\rangle \quad (S3)$$

The normalization of the state,  $\langle\psi|\psi\rangle = 1$ , thus yields  $\int d\mathbf{r}_s d\mathbf{r}_i P(\mathbf{r}_s, \mathbf{r}_i) = 1$ . Explicit expressions for  $P(\mathbf{r}_s, \mathbf{r}_i)$  and  $\Phi(\mathbf{r}_s, \mathbf{r}_i)$  and their relation to  $\Delta z$ ,  $v$  and  $A$ , will be discussed below under the double-Gaussian approximation. For now, we note by inspection of Eq. (S1) that two-photon amplitude is symmetric to the exchange of the signal and idler photons, i.e.,  $P(\mathbf{r}_s, \mathbf{r}_i) = P(\mathbf{r}_i, \mathbf{r}_s)$  and  $\Phi(\mathbf{r}_s, \mathbf{r}_i) = \Phi(\mathbf{r}_i, \mathbf{r}_s)$ .

The photons then pass through a rotating thin diffuser, which imposes a time-dependent random phase mask  $\phi(\mathbf{r})$  onto each of them. The two-photon state is then given by

$$|\psi\rangle = \int d\mathbf{r}_s d\mathbf{r}_i \sqrt{P(\mathbf{r}_s, \mathbf{r}_i)} \exp(i(\Phi(\mathbf{r}_s, \mathbf{r}_i))) \exp(i(\phi(\mathbf{r}_s) + \phi(\mathbf{r}_i))) |1_{\mathbf{r}_s}, 1_{\mathbf{r}_i}\rangle \quad (S4)$$

Equation (S4) thus describes the quantum state of the signal and idler photons generated via SPDC, undergoing free-space propagation, and finally scattered by a rotating diffuser.

### Second-order coherence function

Obtaining the quantum state after the diffuser (Eq. (S4)), we can now proceed to calculate the second-order coherence function. For convenience, we will consider a measurement over a single dimension, yet the same results can be easily extended to two dimensions.

We begin with the calculation of the second-order coherence function

$$g^{(2)}(\Delta\theta) = \frac{\langle\psi|a_s^\dagger(\theta_1)a_i^\dagger(\theta_2)a_i(\theta_2)a_s(\theta_1)|\psi\rangle}{\langle\psi|a_s^\dagger(\theta_1)a_s(\theta_1)|\psi\rangle\langle\psi|a_i^\dagger(\theta_2)a_i(\theta_2)|\psi\rangle} \quad (S5)$$

where  $a_s(\theta) = \sqrt{\frac{k}{2\pi}} \int dr_s a_s(r_s) \exp(-ik\theta r_s)$  is the annihilation operator for a signal photon with (paraxial) transverse wavevector  $q = k\theta$  at the diffuser's plane.

As the integration time of the measurements is much longer than the typical time scale over which the diffuser rotates, we will be interested in the time-averaged, or equivalently disorder-averaged, results. To this end, it is useful to note that for a diffuser with a sufficiently small correlation width, one can approximate the field-field correlations after the diffuser by (16)

$$\overline{\exp(i(\phi(r) - \phi(r')))} = l\delta(r - r') \quad (S6)$$

where the over-bar denotes temporal averaging and  $l$  is a constant with units of length, which depends on the characteristic length scale of the diffuser.

Using this result and the symmetry for signal-idler exchange discussed earlier, we have

$$\begin{aligned} \overline{g^{(2)}(\Delta\theta)} &= \overline{\langle\psi|a_s^\dagger(\theta_1)a_i^\dagger(\theta_2)a_i(\theta_2)a_s(\theta_1)|\psi\rangle} \\ &= \frac{k^2}{4\pi^2} \int dr_s dr_i dr_s' dr_i' \sqrt{P(r_s, r_i)} \sqrt{P(r_s', r_i')} \exp(i(\Phi(r_s, r_i) \\ &\quad - \Phi(r_s', r_i'))) \overline{\exp(i((\phi(r_s) + \phi(r_i)) - (\phi(r_s') + \phi(r_i'))))} \exp(-ik\theta_1(r_s - r_s') \\ &\quad - ik\theta_2(r_i - r_i')) = \frac{k^2 l^2}{4\pi^2} \int dr_s dr_i P(r_s, r_i) (1 + \exp(-ik\Delta\theta(r_i - r_s))) \quad (S7) \end{aligned}$$

And

$$\begin{aligned}
\overline{\langle \psi | a_s^\dagger(\theta_1) a_s(\theta_1) | \psi \rangle} &= \overline{\langle \psi | a_i^\dagger(\theta_2) a_i(\theta_2) | \psi \rangle} \\
&= \frac{k}{2\pi} \int dr_s dr_i dr'_s \sqrt{P(r_s, r_i)} \sqrt{P(r'_s, r_i)} \overline{\exp(i(\phi(r_s) - \phi(r'_s)))} \exp(i(\Phi(r_s, r_i) \\
&\quad - \Phi(r'_s, r_i))) \exp(-ik\theta_1(r_s - r'_s)) = \frac{kl}{2\pi} \int dr_s dr_i P(r_s, r_i) = \frac{kl}{2\pi} \quad (S8)
\end{aligned}$$

Yielding

$$\overline{g^{(2)}(\Delta\theta)} = 1 + \int dr_+ dr_- P(r_s, r_i) \exp(-i\sqrt{2}k\Delta\theta r_-) \quad (S9)$$

where  $r_\pm = \frac{r_i \pm r_s}{\sqrt{2}}$ .

Defining  $h_-(r_-) = \int dr_+ P(r_s, r_i)$  and its Fourier transform  $\widetilde{h}_-(\sqrt{2}k\Delta\theta)$  we have

$$\overline{g^{(2)}(\Delta\theta)} = 1 + \widetilde{h}_-(\sqrt{2}k\Delta\theta) \quad (S10)$$

From now on, temporal averaging will be implicit in order to simplify the notations.

We note that using the symmetry of  $P(r_s, r_i)$ , Eq. (S9) can be equivalently written as  $g^{(2)}(\Delta\theta) = 1 + \int dr_+ dr_- P(r_s, r_i) \cos(\sqrt{2}k\Delta\theta r_-)$ .

Let us now relate the width of  $g^{(2)}(\Delta\theta)$  to the scale  $d$ , defined in the main text as the average distance between the signal and idler photons at the diffuser's plane. We look at the near-field correlations between the photons  $\langle \psi | a_s^\dagger(r_s) a_i^\dagger(r_i) a_i(r_i) a_s(r_s) | \psi \rangle = P(r_s, r_i)$ , and define

$$d^2 \equiv \int dr_s dr_i (r_s - r_i)^2 P(r_s, r_i) = \int dr_- 2r_-^2 \int dr_+ P(r_s, r_i) = 2 \int dr_- r_-^2 h_-(r_-) \quad (S11)$$

The width of the HBT peak, which is given by the angular width of the Fourier transform of  $h_-(r_-)$ , therefore scales as  $\frac{\lambda}{d}$ .

### First-order coherence function

To compare Eq. (S10) with the expected result from the Siegert relation, we shall now look at the first-order coherence function, given by

$$g^{(1)}(\Delta\theta) = \frac{\langle \psi | a_s^\dagger(\theta_1) a_s(\theta_2) | \psi \rangle}{\sqrt{\langle \psi | a_s^\dagger(\theta_1) a_s(\theta_1) | \psi \rangle \langle \psi | a_s^\dagger(\theta_2) a_s(\theta_2) | \psi \rangle}} \quad (S12)$$

Following a similar calculation, we have

$$g^{(1)}(\Delta\theta) = \frac{1}{l} \int dr_s dr_i dr'_s \sqrt{P(r_s, r_i)} \exp\left(i(\phi(r_s) - \phi(r'_s))\right) \exp\left(i(\Phi(r_s, r_i) - \Phi(r'_s, r_i))\right) \exp(-ik\theta_2 r_s + i\theta_1 r'_s) = \int dr_s dr_i P(r_s, r_i) \exp(-ikr_s \Delta\theta) \quad (S13)$$

As expected from the Van Cittert–Zernike theorem, we obtain that the first order coherence function  $g^{(1)}(\Delta\theta)$  at the far-field of the diffuser, is given by the Fourier transform of the single counts distribution at the diffuser's plane  $h_s(r_s) \equiv \langle \psi | a_s^\dagger(r_s) a_s(r_s) | \psi \rangle = \int dr_i P(r_s, r_i)$ . From this Fourier relation, we conclude that the angular width of  $g^{(1)}(\Delta\theta)$  scales as  $\frac{\lambda}{D}$ , where  $D$  is the width of the single photon distribution, defined in the main text as the source size. Comparing this result with the angular width of  $g^{(2)}(\Delta\theta)$  found above, we conclude that the Siegert relation can hold only when  $|\tilde{h}_s(k\Delta\theta)|^2 = \tilde{h}_-(\sqrt{2}k\Delta\theta)$ . Specifically, the width of the two functions must be the same, meaning that  $d \approx D$  must hold for the Siegert relation to be true.

For an inseparable state, although the Siegert relation does not necessarily hold, a Siegert-like relation of the form  $g^{(2)}(\Delta\theta) = 1 + |\tilde{f}(k\Delta\theta)|^2$  can still be obtained, where  $\tilde{f}(k\Delta\theta) = \sqrt{\tilde{h}_-(\sqrt{2}k\Delta\theta)}$  depends on  $d$  rather than  $D$  for the standard Siegert relation. We therefore obtain a relation between the width of the HBT peak and the size of the equivalent two-photon emitter, rather than the total size of the source.

### Density matrix formalism

In the previous sections, we used a pure-state formalism, and performed the temporal averaging when calculating the expectation values for the coherence functions. Alternatively, we can work in the density matrix formalism, and perform the temporal averaging (disorder averaging) on the state itself. The mixed state formalism is valid when the integration time of the measurement is much longer than the correlation time of the rotating diffuser.

We write

$$\begin{aligned} \hat{\rho} = |\psi\rangle\langle\psi| &= \int dr_s dr_i dr'_s dr'_i \sqrt{P(r_s, r_i)} \sqrt{P(r'_s, r'_i)} \exp\left(i(\Phi(r_s, r_i) - \Phi(r'_s, r'_i))\right) \exp\left(i((\phi(r_s) + \phi(r_i)) - (\phi(r'_s) + \phi(r'_i)))\right) |1_{r_s}, 1_{r_i}\rangle\langle 1_{r'_s}, 1_{r'_i}| \\ &= \int dr_s dr_i \tilde{P}(r_s, r_i) (|1_{r_s}, 1_{r_i}\rangle\langle 1_{r_s}, 1_{r_i}| + |1_{r_s}, 1_{r_i}\rangle\langle 1_{r'_i}, 1_{r_s}|) \quad (S14) \end{aligned}$$

where  $\tilde{P}(r_s, r_i) = l^2 P(r_s, r_i)$ . Of course, all results presented earlier can be equivalently obtained using this formalism as well.

### Double-Gaussian approximation

To get explicit and simple expressions for the first- and second-order coherence functions we use the double-Gaussian approximation for the quantum state of SPDC(31)

$$|\psi\rangle_{DG} \propto \int dq_s dq_i \exp\left(-\frac{(q_s + q_i)^2}{\sigma_1^2}\right) \exp\left(-\frac{(q_s - q_i)^2}{\sigma_2^2}\right) |1_{q_s}, 1_{q_i}\rangle \quad (S15)$$

where  $\sigma_1$  is related the waist of the pump beam at the plane of the crystal by  $\sigma_1 = \frac{2}{\sigma_p}$ , and  $\sigma_2 = \sqrt{\frac{4k_p}{L}}$  where  $L$  is the length of the nonlinear crystal and  $k_p$  is the wavevector of the pump beam inside the crystal.

In this case, one can easily see that  $P(r_s, r_i) \propto \exp\left(-\frac{r_s^2}{2\sigma_+^2(\Delta z)}\right) \exp\left(-\frac{r_i^2}{2\sigma_-^2(\Delta z)}\right)$ , where  $\sigma_-(\Delta z) = \sqrt{2\left(\frac{1}{\sigma_2^2} + \frac{\Delta z^2 \sigma_2^2}{16k^2}\right)}$  and  $\sigma_+(\Delta z) = \sqrt{2\left(\frac{1}{\sigma_1^2} + \frac{\Delta z^2 \sigma_1^2}{16k^2}\right)}$ , and identify  $d = \sqrt{2}\sigma_-(\Delta z)$  and  $D = \frac{\sqrt{\sigma_+^2(\Delta z) + \sigma_-^2(\Delta z)}}{\sqrt{2}}$ .

Substituting the above expression for  $P(r_s, r_i)$  into the first- and second-order coherence functions calculated earlier (Eq. (S10) and (S13)) yields

$$g_{DG}^{(2)}(\Delta\theta) = 1 + \exp\left(-\frac{\sigma_-^2(\Delta z)(\sqrt{2}k\Delta\theta)^2}{2}\right) = 1 + \exp\left(-\frac{d^2(k\Delta\theta)^2}{2}\right) \quad (S16)$$

$$\left|g_{DG}^{(1)}(\Delta\theta)\right|^2 = \exp\left(-\frac{(\sigma_+^2(\Delta z) + \sigma_-^2(\Delta z))(k\Delta\theta)^2}{2}\right) = \exp(-D^2(k\Delta\theta)^2) \quad (S17)$$

Indeed, the Siegert relation,  $g_{DG}^{(2)}(\Delta\theta) = 1 + \left|g_{DG}^{(1)}(\Delta\theta)\right|^2$ , only holds when  $\sigma_+(\Delta z) = \sigma_-(\Delta z)$ , which is always true for a separable state, i.e. for  $\sigma_1 = \sigma_2$ . Thus, in the context of SPDC under the double-Gaussian approximation, spatial entanglement is required for the breaking of the Siegert relation. The role of entanglement is in fact more general, as we show in the following section.

To quantify the role of entanglement in the breaking of the Siegert relation, we can look at the ratio of area of the HBT peak and the area of  $\left|g_{DG}^{(1)}(\Delta\theta)\right|^2$ ,  $W_r = \frac{(\sigma_+^2(\Delta z) + \sigma_-^2(\Delta z))}{2\sigma_-^2(\Delta z)} =$

$\frac{1}{2} \left( \frac{\frac{1}{\sigma_1^2} + \frac{\Delta z^2 \sigma_1^2}{16k^2}}{\frac{1}{\sigma_2^2} + \frac{\Delta z^2 \sigma_2^2}{16k^2}} + 1 \right)$ . Assuming high spatial entanglement, the Schmidt number under the double-Gaussian approximation is given by  $K \approx \frac{1}{4} \frac{\sigma_2^2}{\sigma_1^2}$  (31). Thus, for  $\Delta z = 0$ , we have  $W_r \approx 2 \left( K + \frac{1}{4} \right)$  and a direct relation to the entanglement in the state is observed. We note that for large distances, where  $\Delta z \gg \frac{k}{\sigma_1^2}$  and  $\Delta z \gg \frac{k}{\sigma_2^2}$ , we have  $W_r \approx \frac{1}{8} \left( \frac{1}{K} + 4 \right)$ , and the width of the HBT peak can be smaller by up to a factor of  $\sqrt{2}$  compared with the width of  $|g_{DG}^{(1)}(\Delta\theta)|^2$ . Experimental demonstration of this result is out of the scope of the current work, yet it could be an interesting direction for future studies.

In the intermediate distances, a clear relation to the Schmidt number is not present. We thus plot  $W_r$  as a function of  $\Delta z$  for a crystal of length  $L = 8\text{mm}$  and different pump widths, to obtain better understanding of the result (Fig.S1). Specifically, for  $\Delta z = \frac{4k}{\sigma_1 \sigma_2}$ , there are no correlations at the plane of the diffuser, and the Siegert relation is valid regardless of the Schmidt number.

Therefore, we can conclude that the presence of entanglement is a necessary, yet not a sufficient condition for the breakdown of the Siegert relation under the double-Gaussian approximation.

### Separability criterion

To derive a separability criterion based on the measurement of the HBT peak of thermal biphotons, we begin with considering the most general two-photon separable state (44)

$$\rho = \sum_l p_l |\chi_l\rangle\langle\chi_l|_{signal} \otimes |\Psi_l\rangle\langle\Psi_l|_{idler} \quad (S18)$$

where  $|\chi_l\rangle = \int dr u_l(r) |1_r\rangle$ ,  $|\Psi_l\rangle = \int dr v_l(r) |1_r\rangle$  and  $\sum_l p_l = 1$ .

First, we look at the second-order coherence function at the far-field after passing the photons through a rotating diffuser. As for any observable  $O$ ,  $\langle O \rangle_\rho = \text{Tr}(\rho O) = \sum_l p_l \langle \chi_l, \Psi_l | O | \chi_l, \Psi_l \rangle$ , we have

$$\begin{aligned} g^{(2)}(\Delta\theta) &= 1 + \sum_l p_l \int dr_s dr_i u_l(r_s) v_l(r_i) u_l^*(r_i) v_l^*(r_s) \exp(-ik\Delta\theta(r_i - r_s)) \\ &= 1 + \sum_l p_l \left| \int dr_i u_l^*(r_i) v_l(r_i) \exp(-ik\Delta\theta r_i) \right|^2 \quad (S19) \end{aligned}$$

For  $\Delta\theta = 0$ , at the center of the HBT peak, we obtain

$$g^{(2)}(0) = 1 + \sum_l p_l \left| \int dr_i u_l^*(r_i) v_l(r_i) \right|^2 = 1 + \sum_l p_l |\alpha_l|^2 \quad (S20)$$

where we marked  $\langle u_l(r) | v_l(r) \rangle = \int dr_i u_l^*(r_i) v_l(r_i) = \alpha_l$ . To observe a 2:1 HBT peak,  $|\alpha_l|^2 = 1$  must hold for all  $l$ , meaning that  $u_l(r)$  and  $v_l(r)$  are equal up to a global phase. Therefore, we restrict our discussion to separable states of the form

$$\rho = \sum_l p_l |\chi_l\rangle \langle \chi_l|_{signal} \otimes |\chi_l\rangle \langle \chi_l|_{idler} \quad (S21)$$

For which

$$g^{(2)}(\Delta\theta) = 1 + \sum_l p_l \left| \int dr_i |u_l(r_i)|^2 \exp(-ik\Delta\theta r_i) \right|^2 \quad (S22)$$

Taking the Fourier transform of the HBT peak and using the convolution theorem, we obtain

$$F_{HBT}(r) = F.T. (g^{(2)}(\Delta\theta) - 1) = \sum_l p_l |u_l(r)|^2 * |u_l(-r)|^2 \quad (S23)$$

where  $*$  denotes convolution.

Considering  $F_{HBT}(r)$  as a spatial distribution function, its width squared  $\sigma_{F_{HBT}}^2$  is given by its variance

$$\begin{aligned} \sigma_{F_{HBT}}^2 &= \int dr \sum_l p_l r^2 |u_l(r)|^2 * |u_l(-r)|^2 - \left( \int dr \sum_l p_l r |u_l(r)|^2 * |u_l(-r)|^2 \right)^2 \\ &= \sum_l p_l \int dr r^2 |u_l(r)|^2 * |u_l(-r)|^2 \quad (S24) \end{aligned}$$

Where the last step results from the fact that  $|u_l(r)|^2 * |u_l(-r)|^2$  is a symmetric function of  $r$ . We also note that since both  $|u_l(r)|^2$  and  $|u_l(-r)|^2$  are normalized, their convolution is a normalized function as well, allowing us to determine the width of the function by its variance. As the variance of both  $|u_l(r)|^2$  and  $|u_l(-r)|^2$  is the same and equals  $\sigma_{u,l}^2$ , we have that the variance of the convolution is given via  $\sigma_{F_{HBT}}^2 = 2 \sum_l p_l \sigma_{u,l}^2$ .

We will now show that the right-hand side of Eq. (S24) is also equal to the uncertainty in the relative positions of the signal and idler at the diffuser plane  $\sigma_{r_s-r_i}^2$ . By definition, in  $\sigma_{r_s-r_i}^2 = \int dr_s dr_i (r_s - r_i)^2 P(r_s, r_i) - \left( \int dr_s dr_i (r_s - r_i) P(r_s, r_i) \right)^2$ , where  $P(r_s, r_i) = \langle a_s^\dagger(r_s) a_i^\dagger(r_i) a_i(r_i) a_s(r_s) \rangle_\rho$  is the two-photon spatial distribution at the diffuser plane. Using Eq. (S21) we find

$$P(r_s, r_i) = \sum_l p_l |u_l(r_s)|^2 |u_l(r_i)|^2 \quad (S25)$$

Plugging Eq. (S25) into the definition of  $\sigma_{r_s-r_i}^2$  and using the fact that  $P(r_1, r_2)$  is symmetric to the exchange of  $r_s$  and  $r_i$ , we find that

$$\begin{aligned} \sigma_{r_s-r_i}^2 &= \int dr_s dr_i (r_s - r_i)^2 A(r_s, r_i) \\ &= \sum_l p_l \left[ \int dr_i r_i^2 |u_l(r_i)|^2 + \int dr_s r_s^2 |u_l(r_s)|^2 \right. \\ &\quad \left. - 2 \int dr_i r_i |u_l(r_i)|^2 \int dr_s r_s |u_l(r_s)|^2 \right] \quad (S26) \end{aligned}$$

so that

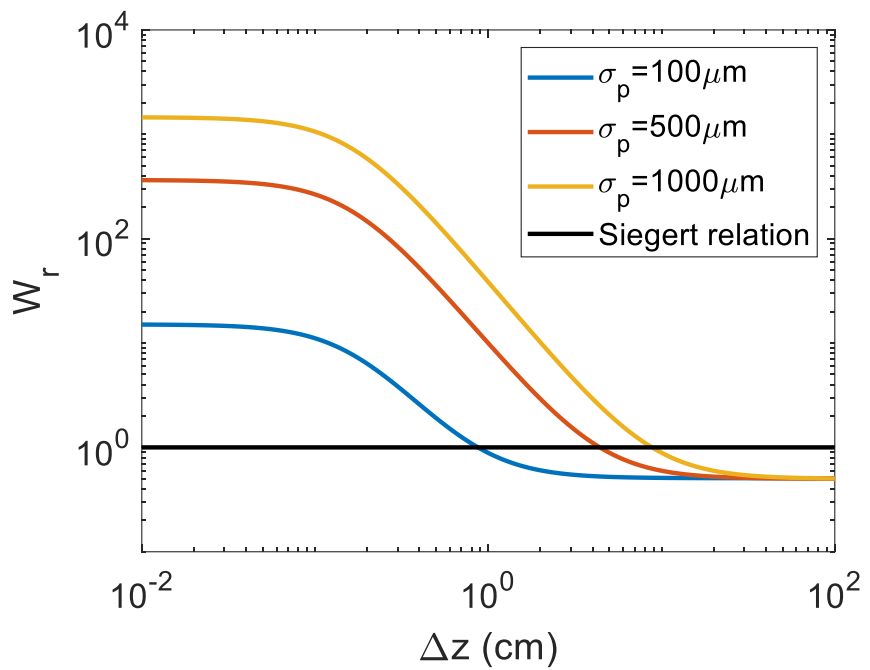
$$\sigma_{r_s-r_i}^2 = 2 \sum_l p_l \sigma_{u,l}^2 = \sigma_{FHBT}^2 \quad (S27)$$

Using Eq. (S27) we can express Mancini's separability criterion (33) by

$$\sigma_{FHBT}^2 \sigma_{k\theta_s+k\theta_i}^2 \geq 1 \quad (S28)$$

Since  $\sigma_{FHBT}^2$  and  $\sigma_{k\theta_s+k\theta_i}^2$  are obtained by measuring the HBT peak and the far-field momentum correlations, both measured at the far-field of the diffuser, we conclude it is possible to certify entanglement of the light hitting the diffuser using a measurement at a single plane.

Fig. S1.



The ratio between the areas of the HBT peak and  $\left|g_{DG}^{(1)}(\Delta\theta)\right|^2$  as a function of  $\Delta z$ , for three different pump widths. The thickness of the nonlinear crystal is  $L = 8\text{mm}$ .